ISSN: 2634 - 6796

Journal of Cardiology Research Reviews & Reports

SCIENTIFIC Research and Community

Research Article

Open Access

Associations of Wall Shear Stress on Vascular Morphology, Hemodynamics, and Many Clinical Variables

Mahashweta Das[1], Ritika Roy Chowdhury[2], Deb Sankar Gupta[3] and Rabindra Nath Das[2*]

[1]Department of History, University of Burdwan, Burdwan, West Bengal, India

[2]Department of Statistics, University of Burdwan, Burdwan, West Bengal, India

[3]Dept. of Agricultural Statistics, Uttar Banga Krishi Viswavidyalaya, Cooch Behar, W.B., India

ABSTRACT

Hemodynamics is generally considered as one of the most important factors in aneurysm rupture. Abnormal wall shear stress, greater pressure and flow impingement are all responsible for aneurysm rupture. The role of wall shear stress on intracranial aneurysms can be identified from its associations with other hemodynamics and related clinical variables, which is very little studied. The report aims to establish the relationship of wall shear stress with other hemodynamics and related clinical variables based on a real data set of 98 aneurysm subjects. It is derived herein that mean wall shear stress (WSS) is marginally positively associated with the subject's diabetes history (DBH) (P<0.001), family history (FMH) (P<0.001), ELAPSS (P<0.001), and it is negatively associated with heart rate (HTR) (P<0.001) & PHASE (P<0.001). Mean WSS is negatively associated with the joint interaction effect (JIE) of age and mean velocity (VEL) i.e., AGE*VEL (P<0.001), JIE of maximum WSS (MXWS) and subject's hypertension history (HPH) i.e., MXWS*HPH (P<0.001), JIE of MXWS and subject's anatomical aneurysm's location (LOC) i.e., MXWS*LOC (P<0.001), JIE of oscillatory shear index (OSI) and maximum pressure (MXPR) i.e. OSI*MXPR (P<0.001), mean WSS gradient (WSG) and mean velocity (VEL) i.e., WSG*VEL (P<0.001), while it is positively associated with the JIEs of mean wall pressure gradient (WPG) and systolic blood pressure (SBP) i.e., WPG*SBP (P<0.001), WPG and subject's smoking history (SMH) i.e., WPG*SMH (P<0.001), OSI*SMH (P<0.001), MXPR*HYP (P<0.001), minimum WSS (MIWS) and subject's alcohol consumption history (ACH) i.e., MIWS*ACH (P<0.001), and many more. These derived associations of WSS with other hemodynamics and related variables may be helpful for the aneurysm rupture treatment process.

***Corresponding author**
Rabindra Nath Das, Department of Statistics, University of Burdwan, Burdwan, West Bengal, India.

Received: September 12, 2025; **Accepted:** September 20, 2025; **Published:** September 30, 2025

Keywords: Aneurysm, Hemodynamics, Hypertension (Hyp), Mean Wall Shear Stress (Wss), Joint Generalized Linear Models (Jglms)

Introduction

Hemodynamics is generally considered as one of the most fundamental factors responsible for aneurysm rupture [1,2]. Several hemodynamic variables/factors such as wall shear stress (WSS), blood flow pattern, mean wall pressure, inlet mass flow etc., are hypothesized to be the causes for aneurysm rupture [3-5]. Intra-aneurysmal stream results in complex stream structure and different stream impinging sites, some at the dome and some at the ostium [6,7]. This complex stream yields a variable WSS distribution on the aneurysm wall. Because WSS determines endothelial functions, understanding of WSS distribution on the aneurysm wall becomes very important [5-7].

Current improvement of numerical tools has enabled us to understand hemodynamics in realistic patient aneurysm geometries [6, 8, 9]. Recent research studies are based on patient-specific aneurysm models that are benefited greatly by advanced 3D angiography as 3D images receive detailed anatomic features, which are generally neglected in idealized geometry [8,10,11]. Although advances in neuroimaging and endovascular treatment have contributed to resolution of many ruptured aneurysms in the stratospheric utilization of resource allocation, predicting which aneurysms will rupture, and subsequently allowing intervention prior to this occurs, remains clinically difficult [10-12]. WSS has emerged as one of the major determinants of aneurysm behaviour [3-5]. Low WSS environments have been shown to induce endothelial cell dysfunction leading to inflammatory infiltration and wall remodeling and degradation within the aneurysmal sac resulting in the potential for ultimate rupture [8,12], while on the other hand, high WSS has been correlated with aneurysm formation and again the role that hemodynamics plays in the underlying pathophysiology of aneurysm is quite complex [2,10,13]. Recently machine learning is increasingly adopted in aneurysm research studies, focusing on factors such as morphology, hemodynamics, and clinical parameters [14-16].

Several articles have focused on the effects of WSS on unruptured and ruptured intracranial aneurysms at the internal carotid artery [3, 6, 9, 14-16], using 3D image analyses, machine learning and other statistical techniques. Image segmentation and aneurysm construction model techniques using 3D images are well discussed in [3,9,11]. Some articles have studied the association of hemodynamic variables/ factors and cerebral aneurysm rupture [3, 9,10, 12], using statistical analysis by 2×2 contingency tables, 2×2 Pearson uncorrected test, etc. In practice, hemodynamic data sets are correlated heteroscedastic and physiological. So, the usual 2×2 contingency tables, 2×2 Pearson uncorrected test, simple or multiple regression analysis are irrelevant. Advanced statistical models such as generalized linear models, joint generalized linear models (JGLMs) are appropriate for analysis of these correlated heteroscedastic physiological data sets. Based on the current literature of hemodynamic data set analyses, it is noted that advanced statistical data analysis techniques are very little used to establish the associations of hemodynamic variables/ factors with the other factors or variables. So, most of the earlier hemodynamic associations' reports invite many debates and doubts. In addition, the previous hemodynamic associations' reports do not use any appropriate model fitting diagnostic tools, which may be doubtful. The associations of mean WSS with other hemodynamic and related variables of aneurysm rupture patients are very few investigated based on probabilistic modeling. The current report investigates the following research hypotheses.

- Is there any association of mean WSS with other hemodynamic and related variables of aneurysm rupture patients ?
- If it is affirmative, how can we derive the most probable mean WSS association model?
- What is the most probable mean WSS statistical model? What are the effects of mean WSS on the other hemodynamic and related variables of aneurysm subjects?

The current article examines the above research hypotheses related to mean WSS considering the following sections such as materials & methods for WSS data analysis, statistical analysis & results of WSS data, discussions, and conclusions of WSS data analysis. The derived WSS joint mean & variance models are shown in Table 2 using the considered hemodynamic data set that is reported in the materials section. The statistical WSS mean-variance models are developed by joint generalized linear models (JGLMs), which is shortly reported in the methods section. The current derived outcomes of WSS data analysis are illustrated in the results section, while their interpretations are reported in the discussion section. From the derived WSS model, the basic hidden information of WSS associations with the other hemodynamic and other related variables is noted in the conclusion section.

Materials and Methods

Materials

The present WSS joint statistical mean & variance model has been obtained from a data set with clinical morphological and hemodynamic variables, which was collected by Song, [17]. A detailed description and the data collection method using 3D models is given in [17]. The data set was collected on 98 aneurysm subjects, and it is available in the site: https://www.kaggle.com/datasets/amirmmahdavikia/cmha-control/code It is well known that intracranial aneurysm is a general life-threatening disease, with a rupture executing to aneurysmal subarachnoid hemorrhage (SAH) and along with a mortality rate exceeding 40% [18]. The progression and rupture of aneurysms is a longstanding research focus, which is associated with vascular morphology, hemodynamics, and many clinical factors, such as aging, gender, hypertension, smoking, diabetes, alcohol use, cerebrovascular disease history, and family SAH history [18, 19]. The current data set contains most of the variables which is clearly presented in [17]. and shortly described in Table 1.

Table 1: Variables Description, their Operationalization & Descriptive Statistics

Variable Name	Operationalization	Minimum	Maximum	Mean	Standard deviation	Proportion (Or %)
Gender (GEN)	Gender of the patient (1 = Male; 2=Female)	1.000	2.000	1.704	0.456	1 = 29.59%; 2 = 70.41%
Age (AGE)	Age of the patient in years	29.00	82.0	59.90	10.310	---------------
Systolic blood pressure (SBP)	Systolic pressure of the patient	87.00	220.0	152.9	26.276	---------------
Diastolic blood pressure (DBP)	Diastolic pressure of the patient	52.00	125.0	89.15	13.351	---------------
Heart Rate (HTR)	Heart rate of the patient, measured in beats per minute (bpm)	53.00	159.0	80.84	13.717	---------------
Respiratory Rate (RER)	Respiratory rate of the patient	13.00	32.00	19.76	2.236	---------------
Smoking History (SMH)	0 = No; 1 = Yes	0.000	1.000	0.051	0.220	0 = 94.90%; 1 = 5.10%
Alcohol Consumption (ACH)	0 = No; 1 = Yes	0.000	1.000	0.071	0.257	0 = 92.86%; 1 = 7.14%
Diabetes History (DBH)	0 = No; 1 = Yes	0.000	1.000	0.092	0.288	0 = 90.82%; 1 = 9.18%
Hypertension History (HPH)	0= No; 1= Yes	0.000	1.000	0.673	0.468	0 = 32.65%; 1 = 67.35%
Family History (FMH)	0 = No; 1 = Yes	0.000	1.000	0.020	0.141	0 = 97.96%; 1 = 2.04%
Has aneurysm	0 = No; 1 = Yes	1.000	1.000	1.000	0	0 = 0%; 1 = 100%
Rupture (RUP)	0 = No; 1 = Yes	0.000	1.000	0.755	0.430	0 = 24.49%; 1 = 75.51%

Shape (SHP)	Morphological shape of the aneurysm (0 =No;1 = Yes)	0.000	1.000	0.663	0.472	0 = 33.67%; 1 = 66.33%
Location (LOC)	1 = M1; 2 = M2	1.000	2.000	1.633	0.482	1 = 36.73%; 2 = 63.27%
Earlier SAH from another aneurysm	0 = No; 1 = Yes	0.000	0.000	0.000	0	0= 100%; 1 = 0%
PHASE	(Population, Hypertension, Age, Size, Earlier SAH) risk scoring system (0-4)	0.0000	4.000	2.122	0.793	---------------
ELAPSS	(Earlier SAH, Location, Age, Population, Size and Shape) scoring system (4-6)	4.000	6.000	4.827	0.429	---------------
Inlet Mass Flow (IMF)	[kg s^{-1}] Mass flow rate of blood entering the aneurysm	0.000977	0.01131	0.0045	0.002	---------------
Outlet 1 Mass Flow (O1MF)	[kg s^{-1}] Mass of blood flowing out through the first specified outlet of the vascular model per second	-0.007211	-0.000147	-0.0026	0.002	---------------
Outlet 2 Mass Flow (O2MF)	[kg s^{-1}] Mass of blood flowing out through the second specified outlet of the vascular model per second	-0.007428	-0.000267	-0.00188	0.001	---------------
Max Velocity (MXVE)	[m/s] Maximum blood flow velocity within the aneurysmal region	0.6351	3.475	1.477	0.6066	---------------
Mean Velocity (VEL)	[m/s] Average blood flow velocity within the aneurysmal region	0.1289	1.212	0.5049	0.180	---------------
Mean Wall Pressure (WPR)	[Pa] Average pressure exerted on the aneurysm walls by the flowing blood	0.4800	17709	13899	1590.923	---------------
Mean Internal Pressure (IPR)	[Pa] Average internal pressure within the blood-filled space of the aneurysm, not necessarily limited to wall regions	13344	18204	14100	832.9108	---------------
Mean wall shear stress (WSS)	[Pa] Tangential force exerted by blood flow on the vessel wall	4.020	56.05	16.10	8.187	---------------
Mean Wall Pressure Gradient (WPG)	[kg m^{-2} s^{-2}] Spatial rate of change of wall pressure	15.92	569339	115331	89886.68	---------------

Mean Internal Pressure Gradient (IPG)	[kg m^{-2} s^{-2}] Spatial rate of change of internal pressure within the aneurysmal volume	6059	959217	126354	121537.7	---------------
Mean WSS Gradient (WSG)	[kg m-2 s-2] Spatial rate of change of WSS over a given distance on the vessel wall	3650	59098	15822	8669.731	---------------
Oscillatory Shear Index (OSI)	Dimensionless number that quantifies the change in direction of wall shear stress during a cardiac cycle	2.053	17.01	5.481	2.161	---------------
Max Pressure (MXPR)	[Pa] Peak pressure in the aneurysmal structure	13547	18914	14654	1092.214	---------------
Max WSS (MXWS)	[Pa] Maximum wall shear stress in the aneurysmal structure	17.92	400.8	90.52	64.799	---------------
Min WSS (MIWS)	[Pa] Lowest wall shear stress in the aneurysmal structure	0.003128	1.054	0.1251	0.1797	---------------
Max Pressure Gradient (MXPG)	[kg m^{-2} s^{-2}] Largest spatial pressure difference recorded in the aneurysmal region	87769	13265000	1377063	1597197	---------------
Max WSS Gradient (MXWSG)	[kg m-^{2} s^{-2}] Maximum change in WSS over aneurysmal space	9276	1674660	247866	263956.409	---------------

Statistical Methods

The current study considers mean wall shear stress (WSS) is the aimed response random variable that is to be modeled with the remaining 34 vascular morphology, hemodynamics, and many clinical factors. It is examined that the response WSS is non-normally and heteroscedastic distributed random variable. The variance of WSS values can't be stabilized with the help of any suitable transformation, therefore it is modeled in the current article using joint generalized linear models (JGLMs) under both the gamma and log-normal distribution that is clearly described in [20-22]. A detailed discussion about JGLMs is given in the book by Lee, Nelder and Pawitan [20]. JGLMS for both the log-normal and gamma distribution are shortly reported herein.

$V(\mu_i)$

Jglms for Log-Normal Distribution: For the positive response Y_i (=WSS) with E(Yi=WSS) = μi (mean) and Var(Yi=WSS) = σ_i^2 μi^2 = say, where σ_i^2's are dispersion parameters and V(.)reveals the variance function. Generally, log transformation Zi = log(Yi=WSS) is adopted to stabilize the variance Var(Zi) ≈σ_i^2, but the variance may not always be stabilized [23]. For developing a WSS improved model, JGLMs for the mean and dispersion are considered. For the response WSS, assuming log-normal distribution, JGL mean and dispersion models (with Zi = log(Yi=WSS)) are as follows:

E(Zi)= μzi and Var(Zi) = σ_{zi}^2,
μzi=xit β and log (σ_{zi}^2)= gi^t γ,
where x_i^t and git are the explanatory factors/variables vectors of WSS associated with the mean regression coefficients β and dispersion regression coefficients γ, respectively.

Jglms for Gamma Distribution: In the above stated Y_i's (=WSS), the variance has two portions such as $V(\mu_i)$ (based on the mean parameters μi's) and σ_i^2 (free of μi's). The variance function V (.) displays the GLM family distributions. For instance, if V(μ)= 1, it is normal, Poisson if V(μ) = , and gamma if V(μ) = etc. Gamma JGLMs mean and dispersion models of GLU are as follows:
and dispersion models of GLU are as follows:

$$\eta_i = g(\mu_i) = x_i^t \beta \text{ and } \varepsilon_i = h(\sigma_i^2) = w_i^t \gamma$$

where and are the GLM link functions attached with the mean and dispersion linear predictors respectively, and x_i^t, w_i^t are the explanatory factors/variables vectors of WSS attached with the mean and dispersion parameters respectively. Maximum likelihood (ML) method is used for estimating the mean parameters, while the restricted ML (REML) method is applied for estimating the dispersion parameters, which are explicitly stated in the book by Lee, Nelder and Pawitan [20].

Statistical analysis & Results

Statistical Analysis

The report aims to derive the associations of WSS on the remaining 34 vascular morphology, hemodynamics, and many clinical variables/factors Probabilistic model of WSS levels has been derived on the remaining 34 explanatory variables (Table 1). Final WSS values model has been accepted based on the lowest Akaike information criterion (AIC) value (within each class) that reduces both the squared error loss and predicted additive errors [24, p. 203--204]. Based on the AIC rule, JGLMs Gamma fit (AIC= -18.575) is identical with the Log-normal fit (AIC=-18.4), as the AIC difference is less than 1 (one). Both the models give similar outcomes. Table 2 displays the summarized JGLMs results of the WSS values analysis of both the mean & variance models under both the Log-normal and Gamma distribution.

Here both the models are identical, so the results of the Gamma model are examined and illustrated. In the mean model of WSS, only two marginal insignificant factors such as alcohol consumption (ACH) (P=0.956) and minimum WSS (MIWS) (P=0.741) are included in the mean model as their joint interaction effect MIWS*ACH (P<0.001) is significant. They are included in the mean model following the marginality rule of Nelder [25], which states that if any higher order interaction effect is significant, then all its lower order interaction effects and marginal effects should be included in the model. In the dispersion model, only one partial significant effect outer 2 mass flow (O2MF) (P=0.232) is included for better fitting.

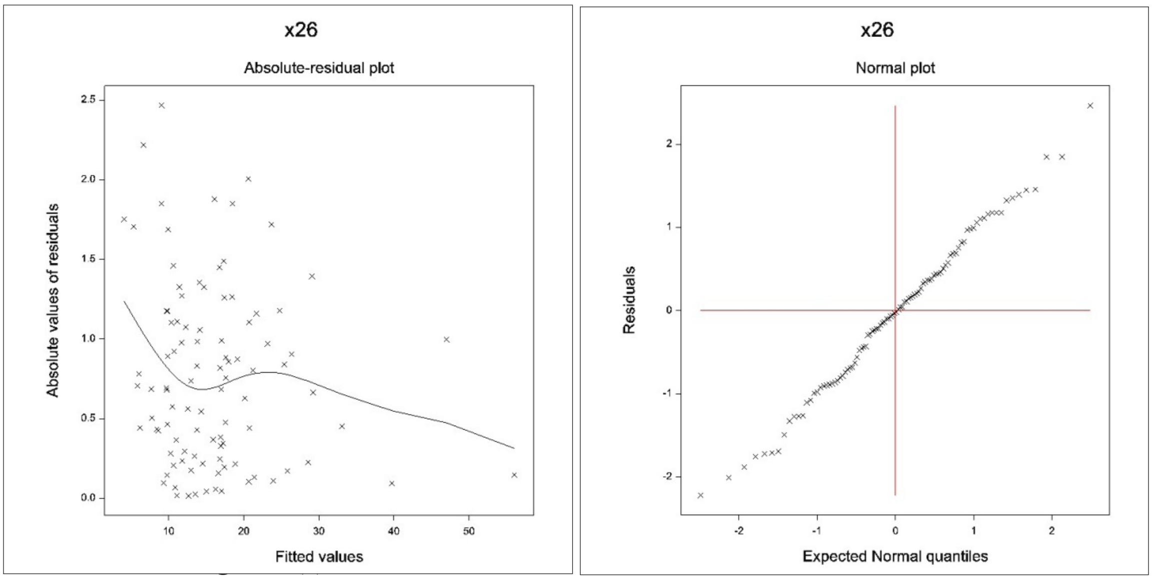

Figure 1: For the joint Gamma fitted models of Wall Shear Stress (Table 2), the (a) absolute residuals plot with the fitted values, and (b) the normal probability plot for mean model

The derived Gamma fitted WSS values probabilistic JGLM (Table 2) is a data derived model that is to be tested by model checking tools. Note that the valid conclusions about WSS values are obtained from the data derived Gamma fitted WSS values probabilistic model (Table 2) that should be taken based on appropriate graphical diagnostic tools, which is shown in Figure 1. Figure 1(a) presents the absolute residuals plot for the Gamma fitted WSS values model (Table 2) with respect to the fitted values, which is almost flat linear except the right tail, indicating that variance is constant with the running means. Note that the right tail is little decreasing as a smaller absolute residual value is located at the right boundary. Figure 1(b) reveals the normal probability plot for the Gamma fitted WSS values mean model (Table 2) that does not reflect any lack of fit. So, both the figures 1(a) and (1b) do not show any discrepancy in the Gamma fitted WSS values model (Table 2). The above Figure 1(a) and Figure 1(b) confirm that the Gamma fitted WSS values model is an approximate form of the unknown true WSS values model. In addition, Figure 2 presents the Histogram of residuals, which indicates no lack of fit.

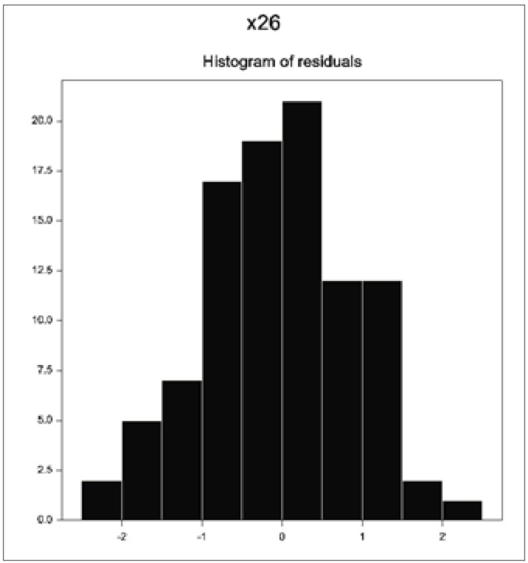

Figure 2: Histogram plot of the joint Gamma fitted residuals of mean Wall Shear Stress (WSS) (Table 2).

Results

The summarized results of WSS values analysis from the both Log-normal and Gamma fitted models are shown in Table 2. According to AIC rules, both the models are almost similar. It is not always true that both the models are similar [26, 27]. The outcomes of the Gamma fitted model (Table 2) are illustrated as follows.

It is derived herein that mean wall shear stress (WSS) is marginally positively associated with the subject's diabetes history (DBH) (P<0.001), family history (FMH) (P<0.001), ELAPSS (P<0.001), and it is negatively associated with heart rate (HTR) (P<0.001) & PHASE (P<0.001).

Mean WSS is negatively associated with the joint interaction effect (JIE) of age and mean velocity (VEL) i.e., AGE*VEL (P<0.001), while both the marginal effects AGE (P=0.006) and VEL (P<0.001) are positively associated with the mean WSS. Mean WSS is negatively associated with the JIE of maximum WSS (MXWS) and subject's hypertension history (HPH) i.e., MXWS*HPH (P<0.001), while it is positively associated with MXWS (P<0.001) and negatively associated with HPH (P<0.001). Mean WSS is negatively associated with the JIE of MXWS and subject's anatomical aneurysm's location (LOC) i.e., MXWS*LOC (P<0.001), while it is positively associated with both the marginal effects MXWS (P<0.001) and LOC (P<0.001). Mean WSS is negatively associated with the JIE of oscillatory shear index (OSI) and maximum pressure (MXPR) i.e., OSI*MXPR (P<0.001), while it is positively associated with the marginal effect MXPR (P<0.001), but it is indifferent of OSI (P=0. 557). Mean WSS is negatively associated with the JIE of mean WSS gradient (WSG) and mean velocity (VEL) i.e., WSG*VEL (P<0.001), while it is positively associated with both the marginal effects WSG (P<0.001) and VEL (P<0.001). Mean WSS is negatively associated with the JIE of mean WSS gradient (WSG) and maximum velocity (MXVE) i.e., WSG*MXVE (P<0.001), while it is positively associated with WSG (P<0.001) and negatively associated with MXVL (P=0.021). Mean WSS is negatively associated with the JIE of maximum velocity (MXVE) and mean internal pressure (IPR) i.e., MXVE*IPR (P<0.001), while it is positively associated with IPR (P<0.001) and negatively associated with MXVL (P=0.021). Mean WSS is negatively associated with the JIE of maximum velocity (MXVE) and mean velocity (VEL) i.e., MXVE*VEL (P<0.001), while it is positively associated with VEL (P<0.001) and negatively associated with MXVL (P=0.021). Mean WSS is negatively associated with the JIE of mean wall pressure (WPR) and maximum pressure gradient (MXPG) i.e., WPR*MXPG (P<0.001), while it is it is negatively associated with WPR (P<0.001) and positively associated with MXPG (P=0.001). Mean WSS is negatively associated with the JIE of oscillatory shear index (OSI) and mean wall pressure gradient (WPG) i.e., OSI*WPG (P<0.0001), while it is negatively associated with WPG (P<0.001) and indifferent of OSI (P=0.557). Mean WSS is negatively associated with the JIE of WSS gradient (WSG) and alcohol consumption (ACH) i.e., WSG*ACH (P<0.001), while it is positively associated with WSG (P<0.001), and it is indifferent of ACH (P=0.956).

On the other hand, mean WSS is positively associated with the JIE of mean wall pressure gradient (WPG) and systolic blood pressure (SBP) i.e., WPG*SBP (P<0.001), while it is negatively associated with both the marginal effects WPG (P<0.001) and SBP (P=0.004). Mean WSS is positively associated with the JIE of wall pressure gradient (WPG) and subject's smoking history (SMH) i.e., WPG*SMH (P<0.001), while it is negatively associated with both the marginal effects WPG (P<0.001) and SMH (P<0.001). Mean WSS is positively associated with the JIE of oscillatory shear index (OSI) and subject's smoking history (SMH) i.e., OSI*SMH (P<0.001), while it is negatively associated with SMH (P<0.001) and indifferent of OSI (P=0.557). Mean WSS is positively associated with the JIE of maximum pressure (MXPR) and the subject's hypertension history (HPH) i.e., MXPR*HPH (P<0.001), while it is negatively associated with HPH (P<0.001) and positively associated with MXPR (P<0.001). Mean WSS is positively associated with the JIE of minimum WSS (MIWS) and subject's alcohol consumption history (ACH) i.e., MIWS*ACH (P<0.001), while it is indifferent of both the marginal effects MIWS (P=0.741) and ACH (P=0.956). Mean WSS is positively associated with the JIE of maximum pressure gradient (MXPG) and location (LOC) i.e., MXPG*LOC (P<0.001), while it is positively associated with both of the marginal effects MXPG (P=0.001) and LOC (P<0.001). Mean WSS is positively associated with the JIE of maximum pressure gradient (MXPG) and maximum pressure (MXPR) i.e., MXPG*MXPR (P<0.001), while it is positively associated with both of the marginal effects MXPG (P=0.001) and MXPR (P<0.001). Mean WSS is positively associated with the JIE of maximum pressure gradient (MXPG) and oscillatory shear index (OSI) i.e., MXPG*OSI (P<0.001), while it is positively associated with the marginal effect MXPG (P=0.001) and indifferent of OSI (P=0.557). Mean WSS is positively associated with the JIE of mean WSS gradient (WSG) and shape (SHP) i.e., WSG*SHP (P<0.001), while it is positively associated with both of the marginal effects WSG (P<0.001) and SHP (P=0.012). Mean WSS is positively associated with the JIE of mean WSS gradient (WSG) and gender (GEN) i.e., WSG*GEN (P<0.001), while it is positively associated with the marginal effect WSG (P<0.001) and negatively associated with GEN (P=0.035). Mean WSS is positively associated with the JIE of oscillatory shear index (OSI) and mean wall pressure (WPR) i.e., OSI*WPR (P<0.001), while it is negatively associated with the marginal effect WPR (P<0.001) and indifferent of OSI (P=0.557). Mean WSS is positively associated with the JIE of maximum WSS gradient (MXWSG) and mean velocity (VEL) i.e. MXWSG*VEL (P<0.001), while it is positively associated with the marginal effect VEL (P<0.001) and negatively associated with MXWSG (P<0.001). Mean WSS is positively associated with the JIE of mean wall pressure gradient (WPG) and mean velocity

(VEL) i.e. WPG*VEL (P=0.001), while it is positively associated with the marginal effect VEL (P<0.001) and negatively associated with WPG (P<0.001). Mean WSS is positively associated with the JIE of mean wall pressure gradient (WPG) and maximum velocity (MXVE) i.e., WPG*MXVE (P<0.001), while it is negatively associated with both of the marginal effects WPG (P<0.001) and MXVE (P=0.021). Mean WSS is positively associated with the JIE of mean wall pressure (WPR) and maximum velocity (MXVE) i.e., WPR*MXVE (P<0.001), while it is negatively associated with both of the marginal effects WPR (P<0.001) and MXVE (P=0.021).

The variance model of WSS is very simple. Variance of WSS is positively associated with shape (SAP) (P=0.002), location (LOC) (P<0.001), outlet 1 mass flow (O1MF) (P<0.001), mean velocity (VEL (P=0.052), while it is partially negatively associated with outlet 2 mass flow (O2MF) (P=0.232).

From Table 2, Gamma fitted WSS values mean ($\hat{\mu}$) model is $\hat{\mu}$ = exp (4.501 + 0.033 Diabetes History - 0.001 Max WSS Gradient + 0.123 Family History + 0.001 Max Pressure Gradient +0.122 Location + 0.001 Max Pressure Gradient*Location – 0.005 Min WSS – 0.002 Alcohol Consumption + 6.320 Min WSS*Alcohol Consumption + 0.022 Max WSS – 0.004 Max WSS*Location – 2.117 Hypertension History – 0.001 Max WSS*Hypertension History + 0.001 Max Pressure + 0.001 Max Pressure Gradient*Max Pressure + 0.001 Max Pressure*Hypertension History -0.061 Oscillatory Shear Index – 0.465 Smoking History + 0.055 Oscillatory Shear Index*Smoking History – 0.001 Max Pressure*Oscillatory Shear Index + 0.001 Max Pressure Gradient*Oscillatory Shear Index + 0.001 Mean WSS Gradient + 0.051 Shape + 0.001 Mean WSS Gradient*Shape – 0.001 Mean WSS Gradient*Alcohol Consumption – 0.050 Gender + 0.001 Mean WSS Gradient*Gender – 0.001 Mean Wall Pressure Gradient – 0.001 Oscillatory Shear Index*Mean Wall Pressure Gradient + 0.001 Mean Wall Pressure Gradient*Smoking History – 0.003 Mean Wall Pressure – 0.001 Max Pressure Gradient*Mean Wall Pressure + 0.001 Oscillatory Shear Index*Mean Wall Pressure + 2.293 Mean Velocity + 0.001 Max WSS Gradient*Mean Velocity – 0.001 Mean WSS Gradient*Mean Velocity + 0.001 Mean Wall Pressure Gradient*Mean Velocity – 1.619 Max Velocity – 0.001 Mean WSS Gradient*Max Velocity + 0.001 Mean Wall Pressure Gradient*Max Velocity + 0.002 Mean Internal Pressure – 0.001 Max Velocity*Mean Internal Pressure + 0.002 Mean Wall Pressure*Max Velocity – 1.123 Mean Velocity*Max Velocity + 0.099 ELAPSS – 0.119 PHASE – 0.002 Heart Rate – 0.001 Systolic + 0.001 Mean Wall Pressure Gradient*Systolic + 0.004 Age – 0.010 Mean Velocity*Age)

and from Table 2, the Gamma fitted WSS values variance $\hat{\sigma}^2$ model is

$\hat{\sigma}^2$ = exp (-10.2 + 1.3 Shape + 2.0 Location + 633.2 Outlet 1 Mass Flow – 217.0 Outlet 2 Mass Flow + 2.9 Mean Velocity) .

Table 1: Results for Mean and Dispersion Models for Mean Wall Shear Stress (Wss) from Log-Normal & Gamma Fit.

Model	Covariates	Gamma fit				Log-normal fit			
		Estimate	Standard error	t-value	P-value	Estimate	Standard error	t-value	P-value
Mean	Constant	4.501	1.174	3.83	<0.001	4.556	1.175	3.87	<0.001
	Diabetes History	0.033	0.009	3.69	<0.001	0.033	0.009	3.72	<0.001
	Max WSS gradient	-0.001	0.001	-4.97	<0.001	-0.001	0.001	-5.00	<0.001
	Family History	0.123	0.018	6.63	<0.001	0.124	0.018	6.64	<0.001
	Max Pressure Gradient	0.001	0.001	3.40	0.001	0.001	0.001	3.42	0.001
	Location	0.122	0.015	7.66	<0.001	0.122	0.015	7.65	<0.001
	Max Pressure Gradient *Location	0.001	0.001	7.93	<0.001	0.001	0.001	7.94	<0.001
	Min WSS	-0.005	0.016	-0.33	0.741	-0.005	0.016	-0.32	0.750
	Alcohol Consumption	-0.002	0.035	-0.06	0.956	-0.002	0.035	-0.05	0.955
	Min WSS * Alcohol Consumption	6.320	0.672	9.40	<0.001	6.350	0.672	9.44	<0.001
	Max WSS	0.022	0.001	22.83	<0.001	0.022	0.001	22.90	<0.001
	Max WSS * Location	-0.004	0.001	-8.84	<0.001	-0.005	0.001	-8.86	<0.001
	Hypertension History	-2.117	0.271	-7.80	<0.001	-2.12	0.271	-7.83	<0.001
	Max WSS * Hypertension History	-0.001	0.001	-4.89	<0.001	-0.001	0.001	-4.91	<0.001
	Max Pressure	0.001	0.001	8.07	<0.001	0.001	0.001	8.10	<0.001

	Max Pressure Gradient * Max Pressure	0.001	0.001	9.75	<0.001	0.001	0.001	9.77	<0.001
	Max Pressure * Hypertension History	0.001	0.001	8.01	<0.001	0.001	0.002	8.04	<0.001
	Oscillatory Shear Index	-0.061	0.102	-0.59	0.557	-0.059	0.102	-0.58	0.565
	Smoking History	-0.465	0.073	-6.32	<0.001	-0.464	0.074	-6.29	<0.001
	Oscillatory Shear Index * Smoking History	0.055	0.010	5.29	<0.001	0.055	0.010	5.31	<0.001
	Max Pressure * Oscillatory Shear Index	-0.001	0.001	-12.4	<0.001	-0.001	0.001	-12.5	<0.001
	Max Pressure Gradient * Oscillatory Shear Index	0.001	0.001	5.51	<0.001	0.001	0.001	5.55	<0.001
	Mean WSS Gradient	0.001	0.001	12.17	<0.001	0.001	0.001	12.22	<0.001
	Shape	0.051	0.019	2.60	0.012	0.051	0.020	2.61	0.012
	Mean WSS Gradient * Shape	0.001	0.001	4.77	<0.001	0.001	0.001	4.78	<0.001
	Mean WSS Gradient * Alcohol Consumption	-0.001	0.001	-10.9	<0.001	-0.001	0.001	-10.9	<0.001
	Gender	-0.050	0.023	-2.17	0.035	-0.051	0.023	-2.22	0.031
	Mean WSS Gradient * Gender	0.001	0.001	4.64	<0.001	0.001	0.001	4.69	<0.001
	Mean Wall Pressure Gradient	-0.001	0.001	-6.06	<0.001	-0.001	0.001	-6.09	<0.001
	Oscillatory Shear Index * Mean Wall Pressure Gradient	-0.001	0.001	-9.44	<0.001	-0.001	0.001	-9.45	<0.001
	Mean Wall Pressure Gradient * Smoking History	0.001	0.001	4.01	<0.001	0.001	0.001	4.01	<0.001
	Mean Wall Pressure	-0.003	0.004	-8.02	<0.001	-0.003	0.001	-8.07	<0.001
	Max Pressure Gradient * Mean Wall Pressure	-0.001	0.001	-7.83	<0.001	-0.001	0.001	-7.86	<0.001

	Oscillatory Shear Index * Mean Wall Pressure	0.001	0.002	10.30	<0.001	0.001	0.001	10.34	<0.001
	Mean Velocity	2.293	0.215	10.63	<0.001	2.29	0.216	10.62	<0.001
	Max WSS Gradient * Mean Velocity	0.001	0.001	5.10	<0.001	0.001	0.001	5.12	<0.001
	Mean WSS Gradient * Mean Velocity	-0.001	0.001	-5.26	<0.001	-0.001	0.001	-5.29	<0.001
	Mean Wall Pressure Gradient * Mean Velocity	0.001	0.001	3.41	0.001	0.001	0.001	3.45	0.001
	Max Velocity	-1.619	0.677	-2.39	0.021	-1.65	0.677	-2.44	0.018
	Mean WSS Gradient * Max Velocity	-0.001	0.001	-11.8	<0.001	-0.001	0.001	-11.94	<0.001
	Mean Wall Pressure Gradient * Max Velocity	0.001	0.001	7.53	<0.001	0.001	0.001	7.55	<0.001
	Mean Internal Pressure	0.002	0.003	7.85	<0.001	0.002	0.003	7.90	<0.001
	Max Velocity * Mean Internal Pressure	-0.001	0.001	-7.32	<0.001	-0.001	0.001	-7.37	<0.001
	Mean Wall Pressure * Max Velocity	0.002	0.002	6.76	<0.001	0.002	0.002	6.81	<0.001
	Mean Velocity * Max Velocity	-1.123	0.091	-12.2	<0.001	-1.124	0.092	-12.2	<0.001
	ELAPSS	0.099	0.015	6.71	<0.001	0.099	0.015	6.72	<0.001
	PHASE	-0.119	0.015	-7.52	<0.001	-0.120	0.016	-7.53	<0.001
	Heart Rate	-0.002	0.002	-7.19	<0.001	-0.002	0.002	-7.23	<0.001
	Systolic	-0.001	0.001	-3.05	0.004	-0.001	0.002	-3.04	0.004
	Mean Wall Pressure Gradient * Systolic	0.001	0.001	4.08	<0.001	0.001	0.001	4.10	<0.001
	Age	0.004	0.001	2.90	0.006	0.003	0.001	2.92	0.005
	Mean Velocity * Age	-0.010	0.002	-3.55	<0.001	-0.009	0.002	-3.59	<0.001
Dispersion	Constant	-10.2	0.74	-13.7	<0.001	-10.2	0.74	-13.7	<0.001
	Shape	1.3	0.40	3.22	0.002	1.3	0.40	3.178	0.003
	Location	2.0	0.41	5.03	<0.001	2.1	0.41	5.05	<0.001
	Outlet 1 Mass Flow	633.2	168.04	3.76	<0.001	626.2	168.06	3.72	<0.001
	Outlet 2 Mass Flow	-217.0	179.10	-1.21	0.232	-222.5	178.81	-1.24	0.220
	Mean Velocity	2.9	1.46	1.992	0.052	2.9	1.46	1.97	0.054

Discussions

The summarized mean WSS values analysis outcomes are presented in Table 2. From Table 2, the most appropriate WSS values Gamma fitted mean and variance models are displayed in the above results section. It is noted in the result section that a few effects are only marginally associated with WSS, while most of the effects are jointly associated with WSS. Marginal effects can be easily explained, while the joint effects indicate their joint functional role on the response variable. This paragraph shows the association of the marginal effects of some explanatory variables of WSS. It is derived herein that mean wall shear stress (WSS) is marginally positively associated with the subject's diabetes history (DBH) (0= No; 1= Yes) (P<0.001), implying that the aneurysm subjects with diabetes history have higher WSS pressure than normal. Mean WSS is marginally positively associated with the subject's family history (0= No; 1=Yes) (FMH) (P<0.001), indicating that WSS pressure is higher for the subjects with family aneurysm history than normal. Mean WSS is marginally positively associated with ELAPSS (P<0.001), concluding that WSS pressure increases as ELAPSS increases. Mean WSS is marginally negatively associated with heart rate (HTR) (P<0.001), interpreting that WSS pressure increases as the subject's heart rate decreases. Mean WSS is marginally negatively associated with PHASE (P<0.001) values, implying that WSS pressure increases as the subject's PHASE values decrease.

It is important to note that if the joint effect is significant, then the marginal effects are not so important. Therefore, for the joint effects, only the functional role of the joint effects will be reported herein. Mean WSS is negatively associated with the JIE of age and mean velocity (VEL) i.e., AGE*VEL (P<0.001), while both the marginal effects AGE (P=0.006) and VEL (P<0.001) are positively associated with the mean WSS. This indicates that WSS pressure increases as the joint effect of AGE*VEL decreases. From the marginal effects, it is noted that at older age and higher mean velocity, WSS pressure should be higher, but it may not be higher as their joint effect AGE*VEL is negatively associated with WSS.

Mean WSS is negatively associated with the JIE of maximum WSS (MXWS) and subject's hypertension history (HPH) i.e., MXWS*HPH (P<0.001), while it is positively associated with MXWS (P<0.001) and negatively associated with HPH (P<0.001). This implies that WSS pressure increases as the joint effect of MXWS*HPH decreases. Aneurysm subjects with higher MXWS pressure and lower hypertension should have higher WSS pressure, but it may not be higher as their joint effect MXWS*HPH is negatively associated with WSS. Mean WSS is negatively associated with the JIE of MXWS and subject's anatomical aneurysm's location (LOC) i.e., MXWS*LOC (P<0.001), while it is positively associated with both the marginal effects MXWS (P<0.001) and LOC (1 = M1; 2 = M2) (P<0.001). This shows that WSS pressure increases as the joint effect of MXWS*HPH decreases.

Mean WSS is negatively associated with the JIE of oscillatory shear index (OSI) and maximum pressure (MXPR) i.e., OSI*MXPR (P<0.001), while it is positively associated with the marginal effect MXPR (P<0.001), but it is indifferent of OSI (P=0.557). This implies that WSS pressure increases as the joint effect of OSI*MXPR decreases. From the marginal effects, it is noted that if MXPR is higher, but WSS pressure may not be higher as the joint effect OSI*MXPR is negatively associated with WSS. Mean WSS is negatively associated with the JIE of mean WSS gradient (WSG) and mean velocity (VEL) i.e., WSG*VEL (P<0.001), while it is positively associated with both the marginal effects WSG (P<0.001) and VEL (P<0.001). This shows that WSS pressure increases as the joint effect of WSG*VEL decreases. From the marginal effects, it is noted that if both the marginal effects WSG and VEL are at higher levels, WSS pressure should be higher, but it may not be higher as their joint effect WSG*VEL is negatively associated with WSS.

Mean WSS is negatively associated with the JIE of mean WSS gradient (WSG) and maximum velocity (MXVE) i.e., WSG*MXVE (P<0.001), while it is positively associated with WSG (P<0.001) and negatively associated with MXVL (P=0.021). This implies that WSS pressure increases as the joint effect of WSG*MXVE decreases. Note that both the marginal effects are oppositely associated with WSS. So, if WSG is higher, but WSS pressure may not be higher, as their joint effect WSG*MXVE is negatively associated with WSS. Mean WSS is negatively associated with the JIE of maximum velocity (MXVE) and mean internal pressure (IPR) i.e., MXVE*IPR (P<0.001), while it is positively associated with IPR (P<0.001) and negatively associated with MXVL (P=0.021). This indicates that WSS pressure increases as the joint effect of MXVE*IPR decreases. Note that both the marginal effects are oppositely associated with WSS. So, if IPR is higher, but WSS pressure may not be higher, as their joint effect MXVE*IPR is negatively associated with WSS.

Mean WSS is negatively associated with the JIE of maximum velocity (MXVE) and mean velocity (VEL) i.e., MXVE*VEL (P<0.001), while it is positively associated with VEL (P<0.001) and negatively associated with MXVL (P=0.021). This indicates that WSS pressure increases as the joint effect of MXVE*VEL decreases. Here both the marginal effects MXVE and VEL are oppositely associated with WSS. So, if VEL is higher, but WSS pressure may not be higher, as their joint effect MXVE*VEL is negatively associated with WSS. Mean WSS is negatively associated with the JIE of mean wall pressure (WPR) and maximum pressure gradient (MXPG) i.e., WPR*MXPG (P<0.001), while it is it is negatively associated with WPR (P<0.001) and positively associated with MXPG (P=0.001). This implies that WSS pressure increases as the joint effect of WPR*MXPG decreases. Here both the marginal effects WPR and MXPG are oppositely associated with WSS. Therefore, for higher MXPG values, WSS pressure may not be higher, as their joint effect WPR*MXPG is negatively associated with WSS.

Mean WSS is negatively associated with the JIE of oscillatory shear index (OSI) and mean wall pressure gradient (WPG) i.e., OSI*WPG (P<0.0001), while it is negatively associated with WPG (P<0.001) and indifferent of OSI (P=0.557). This implies that WSS pressure increases as the joint effect of OSI*WPG decreases. Here the marginal effect WPG and the joint effect OSI*WPG both are negatively associated with WSS, so the joint effect OSI*WPG will be lower, implying WSS pressure will be increasing. Mean WSS is negatively associated with the JIE of WSS gradient (WSG) and alcohol consumption (ACH) i.e., WSG*ACH (P<0.001), while it is positively associated with WSG (P<0.001), and it is indifferent of ACH (P=0.956). This implies that WSS pressure increases as the joint effect of WSG*ACH decreases. Note that the marginal effect WSG and the joint effect WSG*ACH are oppositely associated with WSS, so WSG*ACH will not be lower, consequently, WSS pressure will not be increasing.

In addition, mean WSS is positively associated with the JIE of mean wall pressure gradient (WPG) and systolic blood pressure

(SBP) i.e., WPG*SBP (P<0.001), while it is negatively associated with both the marginal effects WPG (P<0.001) and SBP (P=0.004). This indicates that WSS pressure increases as the joint effect WPG*SBP increases. Both the marginal effects (WPG & SBP) and WPG*SBP are oppositely associated with WSS, so the joint effect WPG*SBP will not be too high, consequently, WSS pressure will not be increasing due to the joint effect WPG*SBP. Mean WSS is positively associated with the JIE of wall pressure gradient (WPG) and subject's smoking history (SMH) i.e., WPG*SMH (P<0.001), while it is negatively associated with both the marginal effects WPG (P<0.001) and SMH (P<0.001). This implies that WSS pressure increases as the joint effect WPG*SMH increases. Both the marginal effects (WPG & SMH) and WPG*SMH are oppositely associated with WSS, so the joint effect WPG*SMH will not be too high, consequently, WSS pressure will not be increasing due to the joint effect WPG*SMH. Mean WSS is positively associated with the JIE of oscillatory shear index (OSI) and subject's smoking history (SMH) i.e., OSI*SMH (P<0.001), while it is negatively associated with SMH (P<0.001) and indifferent of OSI (P=0.557). This implies that WSS pressure increases as the joint effect OSI*SMH increases. Note that the marginal SMH and the joint effect OSI*SMH are oppositely associated with WSS, so the joint effect OSI*SMH will not be too high, consequently, WSS pressure will not be increasing due to the joint effect OSI*SMH.

Mean WSS is positively associated with the JIE of maximum pressure (MXPR) and the subject's hypertension history (HPH) i.e., MXPR*HPH (P<0.001), while it is negatively associated with HPH (P<0.001) and positively associated with MXPR (P<0.001). This shows that WSS pressure increases as the joint effect MXPR*HPH increases. It is observed herein that (MXPR*HPH & MXPR) and HPH are oppositely associated with WSS, so the joint effect MXPR*HPH will be higher, if the HPH level is lower. Mean WSS is positively associated with the JIE of minimum WSS (MIWS) and subject's alcohol consumption history (ACH) i.e., MIWS*ACH (P<0.001), while it is indifferent of both the marginal effects MIWS (P=0.741) and ACH (P=0.956). This reveals that WSS pressure increases as the joint effect MXPR*HPH increases. Note that both the marginal effects MIWS and ACH are inactive with WSS.

Mean WSS is positively associated with the JIE of maximum pressure gradient (MXPG) and location (LOC) i.e., MXPG*LOC (P<0.001), while it is positively associated with both of the marginal effects MXPG (P=0.001) and LOC (P<0.001). This indicates that WSS pressure increases as the joint effect MXPR*LOC increases. Note that both the marginal effects MXPG and LOC are positively associated with WSS. Therefore, these two marginal effects and the joint effect are positively associated with WSS, so for the higher joint effect MXPG*LOC, WSS pressure will be higher. Mean WSS is positively associated with the JIE of maximum pressure gradient (MXPG) and maximum pressure (MXPR) i.e., MXPG*MXPR (P<0.001), while it is positively associated with both of the marginal effects MXPG (P=0.001) and MXPR (P<0.001). This indicates that WSS pressure increases as the joint effect MXPG*MXPR increases. Note that both the marginal effects MXPG and MXPR are positively associated with WSS. Therefore, these two marginal effects and the joint effect are positively associated with WSS, so for the higher joint effect MXPG*MXPR, WSS pressure will be higher. Mean WSS is positively associated with the JIE of maximum pressure gradient (MXPG) and oscillatory shear index (OSI) i.e., MXPG*OSI (P<0.001), while it is positively associated with the marginal effect MXPG (P=0.001) and indifferent of OSI (P=0.557). This implies that WSS pressure increases as the joint effect MXPG*OSI increases. Note that the marginal effect MXPG and the joint effect MXPG*OSI are positively associated with WSS. So, for the higher joint effect MXPG*OSI, WSS pressure will be higher. Mean WSS is positively associated with the JIE of mean WSS gradient (WSG) and shape (SHP) i.e., WSG*SHP (P<0.001), while it is positively associated with both of the marginal effects WSG (P<0.001) and SHP (P=0.012). This implies that WSS pressure increases as the joint effect WSG*SHP increases. Note that both the marginal effects WSG and SHP are positively associated with WSS. Therefore, these two marginal effects and the joint effect are positively associated with WSS, so for the higher joint effect WSG*SHP, WSS pressure will be higher.

Mean WSS is positively associated with the JIE of mean WSS gradient (WSG) and gender (GEN) i.e., WSG*GEN (P<0.001), while it is positively associated with the marginal effect WSG (P<0.001) and negatively associated with GEN (1=male, 2=female) (P=0.035). This indicates that WSS pressure increases as the joint effect WSG*GEN increases. It shows that WSS pressure is higher for male than females. Mean WSS is positively associated with the JIE of oscillatory shear index (OSI) and mean wall pressure (WPR) i.e., OSI*WPR (P<0.001), while it is negatively associated with the marginal effect WPR (P<0.001) and indifferent of OSI (P=0.557). This indicates that WSS pressure increases as the joint effect OSI*WPR increases. Moreover, OSI*WPR and WPR are oppositely associated with WSS, so WSS pressure will not be too high due to the effect OSI*WPR.

Mean WSS is positively associated with the JIE of maximum WSS gradient (MXWSG) and mean velocity (VEL) i.e. MXWSG*VEL (P<0.001), while it is positively associated with the marginal effect VEL (P<0.001) and negatively associated with MXWSG (P<0.001). This indicates that WSS pressure increases as the joint effect MXWSG*VEL increases. In addition, (MXWSG*VEL & VEL) and MXWSG are oppositely associated with WSS, so WSS pressure will not be too high due to the effect MXWSG*VEL. Mean WSS is positively associated with the JIE of mean wall pressure gradient (WPG) and mean velocity (VEL) i.e. WPG*VEL (P=0.001), while it is positively associated with the marginal effect VEL (P<0.001) and negatively associated with WPG (P<0.001). This shows that WSS pressure increases as the joint effect WPG*VEL increases. In addition, (WPG*VEL & VEL) and WPG are oppositely associated with WSS, so WSS pressure will not be too high due to the effect WPG*VEL. Mean WSS is positively associated with the JIE of mean wall pressure gradient (WPG) and maximum velocity (MXVE) i.e., WPG*MXVE (P<0.001), while it is negatively associated with both of the marginal effects WPG (P<0.001) and MXVE (P=0.021). This shows that WSS pressure increases as the joint effect WPG*MXVE increases. Note that both the marginal effects (WPG & MXVE) and the interaction effect WPG*MXVE are oppositely associated with WSS, so WSS pressure will not be too high due to the effect WPG*MXVE. Mean WSS is positively associated with the JIE of mean wall pressure (WPR) and maximum velocity (MXVE) i.e., WPR*MXVE (P<0.001), while it is negatively associated with both of the marginal effects WPR (P<0.001) and MXVE (P=0.021). This shows that WSS pressure increases as the joint effect WPR*MXVE increases. Note that both the marginal effects (WPR & MXVE) and the interaction effect WPG*MXVE are oppositely associated with WSS, so WSS pressure will not be too high due to the effect WPR*MXVE.

The association of variance of WSS is very simple. Variance of WSS is positively associated with shape (SAP) (P=0.002), location (LOC) (P<0.001), outlet 1 mass flow (O1MF) (P<0.001), mean velocity (VEL (P=0.052), these implies that WSS values are highly scattered of the aneurysm subjects with higher values of shape, aneurysm at location M2, with higher values of outlet 1 mass flow and mean velocity.

The associations of WSS with vascular morphology, hemodynamics, and many clinical factors/ variables have been derived herein. It is observed that WSS has a very complicated relationship with these factors. WSS is significantly associated with many marginal and joint interaction effects. Marginal associations are easily understandable, while the joint interaction effects are not so simple. Note that the joint interaction effects on WSS can be identified using only statistical modeling. Best of our knowledge, no earlier article identifies any joint interaction association of WSS. It is derived herein that some marginal effects such as subject's diabetes history, family history, higher ELAPSS values, low heart rate, and low PHASE values etc. are responsible for the higher WSS pressure, while some joint interaction effects such as OSI*WPG, MXPG*LOC, MXPG*MXPR, MXPG*OSI, WSG*SHP etc. are always responsible for higher WSS pressure. Many joint interaction effects are also responsible for higher WSS pressure under some situations.

Conclusions

The present article has developed the associations of WSS pressure with vascular morphology, hemodynamics, and many clinical factors/ variables. The fitted WSS values probabilistic model has been accepted herein based on the smallest AIC rule, graphical diagnostic checking plots (Figure 1 & Figure 2), standard error of the estimates, and on comparison of joint Log-normal and Gamma models. Both the fitted models (Log-normal & Gamma) have similar interpretations (Table 2). Marginal effects on WSS are easily understandable, which reflects the real situations, while the joint effects are very difficult, which are very little pointed in the earlier research articles. Functional activity of different factors on the human body can only be identified by a proper statistical modelling. There is no single instrument in the world which can identify the joint effect of two or more factors together on the human body. The current report has derived an approximate model (Table 2) of WSS, and the derived associations of WSS with vascular morphology, hemodynamics, and many clinical factors or variables though not completely eventual but are expressive. Advanced medical scientific research methods should have complete faith on these derived associations of WSS as the fitted models have been tested with graphical diagnostic checking and comparison of two different models.

For any similar data sets of WSS values with vascular morphology, hemodynamics, and many clinical factors, the findings will be almost similar to the present findings, which are not verified herein as similar data sets are not available. The present associations of WSS reveal many real facts, which are rarely reported in the earlier articles. Most of the associations of WSS in the report are completely new in the hemodynamics study literature. In addition, the report may help all the people, heart patients, medical practitioners and researchers. It is concluded that WSS values have very complex associations (Table 2) with vascular morphology, hemodynamics, and many clinical factors that should be known to the practitioners for appropriate treatment processes.

Declarations: The article is an original interesting research report that has been prepared based on advance statistical data analysis using , which has not been submitted in any journal for publication.

Acknowledgement: The authors are very grateful to the principal data investigators, who provided the data freely for scientific study.

Funding: The authors declare no financial support for the research, authorship, or publication of this article.

Author contributions: Conceptualization, R.D. M.D; methodology, R.D. D.S.G and R.R.C; software, R.D.; validation, R.D. and M.D.; formal analysis, R.D., D.S.G..; investigation, R.D. and M.D..; resources, M.D and R.R.C.; data curation, R.R.C..; writing—original draft preparation, R.D.; writing—review and editing, R.D. and D.S.G.; visualization, R.D. and D.S.G.; supervision, M.D.; project administration, R.D.; funding acquisition, R.D..; All authors have read and agreed to the published version of the manuscript.

Conflict of interest: The authors confirm that this article content has no conflict of interest.

Ethical approval: Note that the current study has been performed based on a secondary data set. The ethics approval and the subject consents are not required for a secondary published data set.

Data Availability Statement

The data is available in the site- https://www.kaggle.com/datasets/amirmmahdavikia/cmha-control/code

Informed consent statement

Not applicable

Sample availability

The authors declare no physical samples were used in the study

Abbreviations

ACH Alcohol Consumption
AIC Akaike information criterion
GEN Gender
DBH Diabetes History
DBP Diastolic blood pressure;
FMH Family History
HPH Hypertension history
HTR Heart rate
IMF Inlet Mass Flow
IPR Mean Internal Pressure
IPG Mean Internal Pressure Gradient
JGLMs Joint generalized linear models
JIE Joint interaction effect
LOC Location
MIWS Min WSS
MXPG Max Pressure Gradient
MXPR Max Pressure
MXVE Max Velocity
MXWS Max WSS
MXWSG Max WSS Gradient
O1MF Outlet 1 Mass Flow
O2MF Outlet 2 Mass Flow
OSI Oscillatory Shear Index
RER Respiratory Rate
RUP Rupture
SBP Systolic blood pressure

SHP Shape
SAH Subarachnoid hemorrhage
SMH Smoking History
WPG Mean Wall Pressure Gradient
WSG Mean WSS Gradient
WPR Mean Wall Pressure
WSS Mean wall shear stress
VEL Mean Velocity

References

1. Hashimoto T, Meng H, Young WL (2006) Intracranial aneurysm. link among inflammation,hemodynamics and vascular remodeling. Neurol Res 28: 372–380.
2. Mutlu O, Salman HE, Al-Thani H, El-Menyar A, Uvais Ahmed Qidwai, et al. (2023) How does hemodynamics affect rupture tissue mechanics in abdominal aortic aneurysm. Focus on wall shear stress derived parameters, time-averaged wall shear stress, oscillatory shear index, endothelial cell activation potential, and relative residence time. Computers in Biology and Medicine 154:106609.
3. Cebral JR, Mut F, Weir J, Putman CM (2011) Association of Hemodynamic Characteristics and Cerebral Aneurysm Rupture. AJNR Am J Neuroradiol 32: 264-270.
4. Jou LD, Lee DH, Morsi H. Mawad ME (2008) Wall Shear Stress on Ruptured and Unruptured Intracranial Aneurysms at the Internal Carotid Artery. AJNR Am J Neuroradiol 29: 1761-1767.
5. Veeturi SS, Patel TR, Baig AA, Chien A, Andre Monteiro, et. al. (2002) Hemodynamic Analysis Shows High Wall Shear Stress Is Associated with Intraoperatively Observed Thin Wall Regions of Intracranial Aneurysms. J Cardiovasc Dev Dis 9 :424.
6. Ma B, Harbaugh RE, Raghavan ML (2004) Three-dimensional geometrical characterizatio of cerebral aneurysms. Ann Biomed Eng 32: 264–273
7. Cebral JR, Castro MA, Burgess JE, Richard S Pergolizzi, Michael J Sheridan, et al. (2005) Characterization of cerebral aneurysms for assessing risk of rupture by using patient-specific computational hemodynamics models. AJNR Am J Neuroradiol 26: 2550-2559
8. ShojimaS M, Oshima M, Takagi K, Ryo Torii, Kazuya Nagata, et al. (2005) Role of the bloodstream impacting force and the local pressure elevation in the rupture of cerebral aneurysms. Stroke 36: 1933-1938.
9. Jou L, Quick C, Young W, Michael T Lawton, Randall Higashida, et al. (2003) Computational approach to quantifying hemodynamic forces in giant cerebral aneurysms. AJNR Am J Neuroradiol 24: 1804-1810.
10. Steinman D, Miller J, Norley C, Stephen P Lownie, David W Holdsworth, et al. (2003) Image-based computational simulation of flow dynamics in a giant intracranial aneurysm. AJNR Am J Neuroradiol 24: 559-564
11. Jou L, Quick C, Young W, Michael T Lawton, Randall Higashida, et al. (2003) Computational approach to quantifying hemodynamic forces in giant cerebral aneurysms. AJNR Am J Neuroradiol 24:1804-1810
12. Shojima M, Oshima M, takagi K, Ryo Torii, Motoharu Hayakawa, et al. (2004) Magnitude and role of wall shear stress on cerebral aneurysm: computational fluid dynamics study of 20 middle cerebral artery aneurysms. Stroke 35: 2500-2505
13. Xiang J, Sabareesh K Natarajan, Markus Tremmel, Ding Ma, J Mocco, et al. (2011) Hemodynamic–morphologic discriminants for intracranial aneurysm rupture. Stroke 42 :144-152.
14. Chung B, F Mut, C M Putman, F Hamzei Sichani, W Brinjikji, et al. (2020) Identification of hostile hemodynamics and geometries of cerebral aneurysms: a case-control study. American Journal of Neuroradiology 39: 1860-1866.
15. Hu S, Li M, YiYun Li, Zheng Hao, et al. (2019) Zheng Liu In reply: a meta-analysis of risk factors for the formation of de novo intracranial aneurysms. Neurosurgery, 85: 454-465
16. Kim H, C Jong Kook Rhim, Jun Hyong Ahn, Jeong Jin Park, Jong Un Moon, et al. (2019) Machine learning application for rupture ris assessment in small-sized intracranial aneurysm. Journal of clinical medicine 8: 683.
17. Song M, Wang S, Qianz Q, Yuan Zhou, Yi Luo, et al. (2024) Intracranial aneurysm CTA images and 3D models data set with clinical morphological and hemodynamic data. Scientific Data, 11: 1213.
18. Rooij De, Linn NK, Van Der Plas FHH, A Algra, G J E Rinkel, et al. (2002) Incidence of subarachnoid haemorrhage: a systematic review with emphasis on region, age, gender and time trends. Journal of Neurology, Neurosurgery & Psychiatry 78: 1365-1372.
19. Shi Z, Chongchang Miao, U Joseph Schoepf, Rock H Savage, Danielle M Dargis, et al. (2020) A clinically applicable deep-learning model for detecting intracranial aneurysm in computed tomography angiography images. Nature communications, 11: 6090.
20. Lee Y, Nelder JA, Pawitan Y (2017) Generalized Linear Models with Random Effects (Unified Analysis via H–likelihood) (Second Edition). London: Chapman & Hall 30: 466
21. Das RN, Lee Y (2009) Log-normal versus gamma models for analyzing data from quality-improvement experiments. Quality Engineering 21: 79-87.
22. Qu Y, Tan M, Rybicki L (2000) A unified approach to estimating association measures via a joint generalized linear model for paired binary data. Communications in Statistics – Theory and Methods 29:143-156.
23. Myers R H, Montgomery D C, Vining G G (2002) Generalized Linear Models with Applications in Engineering and the Sciences. New York: John Wiley & Sons, (2002).
24. Hastie T, Tibshirani R, Friedman J (2001) The Elements of Statistical Learning, Springer-Verlag https://www.sas.upenn.edu/~fdiebold/NoHesitations/BookAdvanced.pdf.
25. Nelder JA (1994) The statistics of linear models: back to basics. Statistics and Computing 4: 221-234.
26. Das RN (2012) Discrepancy in fitting between log-normal and gamma models: An illustration. Model Assisted Statistics and Applications 7: 23-32.
27. Das RN, Park JS (2012) Discrepancy in regression estimates between Log-normal and Gamma: Some case studies. Journal of Applied Statistics 39: 97-111.